BIOCHEMISTRY
including biophysical chemistry & molecular biology

Article

pubs.acs.org/biochemistry

Formation of Oligomeric Cytochrome *c* during Folding by Intermolecular Hydrophobic Interaction between N- and C-Terminal α-Helices

Partha Pratim Parui,[†,‡] Megha Subhash Deshpande,[†] Satoshi Nagao,[†] Hironari Kamikubo,[†] Hirofumi Komori,[§,∥,⊥] Yoshiki Higuchi,[§,∥] Mikio Kataoka,[†] and Shun Hirota*[,†]

[†]Graduate School of Materials Science, Nara Institute of Science and Technology, 8916-5 Takayama, Ikoma, Nara 630-0192, Japan

[‡]Department of Chemistry, Jadavpur University, Kolkata 700032, India

[§]Department of Life Science, Graduate School of Life Science, University of Hyogo, 3-2-1 Koto, Kamigori-cho, Ako-gun, Hyogo 678-1297, Japan

[∥]RIKEN SPring-8 Center, 1-1-1 Koto, Sayo-cho, Sayo-gun, Hyogo 679-5148, Japan

Supporting Information

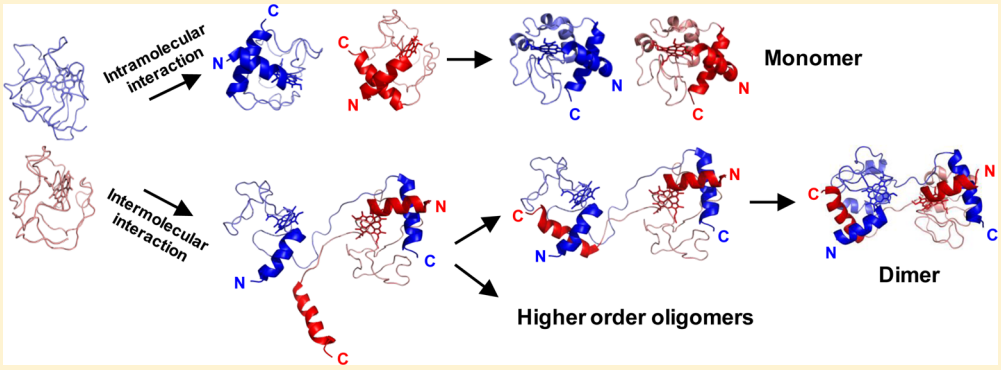

ABSTRACT: We have previously shown that horse cytochrome *c* (cyt *c*) forms oligomers by domain swapping its C-terminal α-helix when interacting with ethanol. Although folding of cyt *c* has been studied extensively, formation of domain-swapped oligomers of cyt *c* during folding has never been reported. We found that domain-swapped oligomeric cyt *c* is produced during refolding from its guanidinium ion-induced unfolded state at high protein concentrations and low temperatures. The obtained dimer exhibited a domain-swapped structure exchanging the C-terminal α-helical region between molecules. The extent of dimer formation decreased significantly for the folding of C-terminal cyt *c* mutants with reduced hydrophobicity achieved by replacement of hydrophobic residues with Gly in the C-terminal region, whereas a large amount of heterodimers was generated for the folding of a mixture of N- and C-terminal mutants. These results show that cyt *c* oligomers are formed through intermolecular hydrophobic interaction between the N- and C-terminal α-helices during folding. A slow phase (4−5 s) was observed in addition to a 400−500 ms phase during folding of a high concentration of cyt *c* in the presence of 1.17 M guanidine hydrochloride. The fast phase is attributed to the intramolecular ligand exchange process, and we attribute the slow phase to the ligand exchange process in oligomers. These results show that it is important to consider formation of domain-swapped oligomeric proteins when folding at high protein concentrations.

Cytochrome *c* (cyt *c*) is a globular heme protein with three long α-helices surrounding its heme.[1−3] Cyt *c* transfers electrons from the cytochrome bc_1 complex to cytochrome *c* oxidase in the respiratory chain in mitochondria. It also plays a key role in apoptosis, where it is released to the cytosol when permeabilization of the mitochondrial outer membrane occurs.[4,5] The heme of cyt *c* forms covalent bonds with two cysteine residues, and His18 and Met80 are coordinated to the heme iron. We have shown that cyt *c* forms polymers by successive domain swapping of the C-terminal α-helix.[6] The C-terminal helix of cyt *c* was displaced from its original position in the monomer, and the Met−heme coordination was perturbed significantly, causing higher peroxidase activity in the dimer than in the monomer.[6,7] It has also been reported that domain-swapped cyt *c* oligomers are formed by exposure of the oxidized monomeric protein to alkaline conditions at high protein concentrations.[8]

Research on proteins showing domain-swapped structures is becoming more frequent,[9−12] and domain-swapped structures have also been reported for amyloidogenic proteins.[13−17]

Received: July 23, 2013
Revised: November 6, 2013
Published: November 8, 2013

dx.doi.org/10.1021/bi400986g | *Biochemistry* 2013, 52, 8732−8744

Oligomerization of RNase A has been studied intensively,[18−20] and it has been shown that RNase A oligomerizes most efficiently at high temperatures, where it is completely denatured.[21,22] Nuclear magnetic resonance spectroscopic studies of RNase A have shown that the protein partially retains the native helices but the β-sheet is fully denatured in 40% acetic acid, and its dimerization occurs from the folding intermediate during the dissolution process of its precipitates.[23] A high activation energy was obtained for formation and/or dissociation of dimeric stefin A, p13suc 1, and cyanovirin-N, suggesting that domain swapping proceeds via complete unfolding.[24−26] The domain-swapped dimer of barnase has been reported to be produced from the same folding intermediate as its monomer.[27] It has been suggested that domain-swapped oligomers of cyanovirin-N are trapped folding intermediates.[28] The heme of horse myoglobin has been shown to dissociate from the protein during formation of its domain-swapped dimer, presumably because of a protein structural change at the active site.[29] Although the formation of domain-swapped oligomers during folding may be a common character of many proteins, the detailed mechanism and interaction responsible for oligomerization remain unknown.

Cyt *c* has served as a model for protein folding. In the folding of oxidized cyt *c*, a hydrophobic collapse of the polypeptide chain occurs with formation of the N- and C-terminal α-helices on a submillisecond time scale,[30−33] followed by coordination of Met80 to the heme iron on a millisecond time scale.[34−37] Approximately 44% of the α-helical signal of native oxidized cyt *c* arose during folding within the dead time of the stopped-flow circular dichroism (CD) measurement, indicating that a significant amount of secondary structure was formed within 4 ms.[38] A transient dimer has been detected during folding of cyt *c* by small-angle X-ray scattering (SAXS) measurements,[39] but its nature remains unknown. In this study, we show that cyt *c* forms domain-swapped oligomers during folding by hydrophobic interaction between the N- and C-terminal α-helices. We also observed a slow kinetic folding phase (4−5 s) at high protein concentrations in the presence of 1.17 M guanidine hydrochloride (GdnHCl) and attributed it to the ligand exchange reaction of oligomeric cyt *c*.

MATERIALS AND METHODS

Plasmids of Wild-Type and Mutant Human Cyt *c*. Human cyt *c* was expressed by coexpressing the cyt *c* and cyt *c* heme lyase (CCHL) genes.[40,41] The human cyt *c* gene was amplified by polymerase chain reaction (PCR) of the pME18SFL3 plasmid containing the human cyt *c* gene (Toyobo, Osaka, Japan) and subcloned into the SmaI−PstI site of the pUC18 plasmid. The cyt *c* heme lyase (CCHL) gene was obtained from the *Saccharomyces cerevisiae* gene (strain ATCC 18824) by PCR. The CCHL gene was subcloned into the PstI−HindIII site of the human cyt *c* gene-containing plasmid, where a lac promoter sequence was placed upstream of the CCHL gene. After digestion of the obtained plasmid with SmaI and HindIII, the fragment containing both human cyt *c* and CCHL genes was subcloned into the SmaI−HindIII site of the pEMBL18+ plasmid.[42] Point mutations were introduced into human cyt *c* by PCR-based *in vitro* mutagenesis of the human cyt *c* expression plasmid using forward and reverse primers (Sigma-Aldrich) (Table S1 of the Supporting Information). Plasmid DNAs were prepared using the QIAprep spin Mini prep kit (Qiagen). DNA sequencing was conducted with the BigDye Terminator version 3.1 cycle sequencing kit (Applied Biosystems, Inc., Foster City, CA) and an ABI PRISM 310 genetic analyzer sequencing system (Applied Biosystems, Inc.). The obtained plasmids were introduced into competent *Escherichia coli* Rosetta2 (DE3) pLysS cells (Novagen).

Purification of Horse and Human Cyt *c*. Oxidized horse heart cyt *c* (Sigma-Aldrich) was purified by cation exchange chromatography with CM52 (Whatman, Springfield Mill, England). Recombinant wild-type (WT) and mutant human cyt *c* proteins were overproduced in *E. coli* Rosetta2 (DE3) pLysS cells. The cells were grown at 37 °C in 25 g/L modified LB broth (3 g/L yeast extract, 2 g/L $NaNO_3$, and 1.5 mL/L glycerin) until the OD_{600} reached 1.2−1.5. Cells were harvested by centrifugation and suspended in a minimal volume of 50 mM potassium phosphate buffer (pH 7.0). The obtained cyt *c* solution was dialyzed overnight in 5 mM potassium phosphate buffer (pH 7.0). Cyt *c* was purified via cation exchange chromatography with CM52 (Whatman) and subsequently via gel chromatography (Hiload 26/60 Superdex 75, GE Healthcare, Buckinghamshire, England) using a fast performance liquid chromatography (FPLC) system (BioLogic DuoFlow 10, Bio-Rad, Hercules, CA) [flow rate of 0.8 mL/min, monitoring wavelength of 415 nm, solvent of 50 mM potassium phosphate buffer (pH 7.0), and temperature of 4 °C]. Oxidized cyt *c* was obtained via the addition of a potassium ferricyanide (Sigma-Aldrich) solution and the subsequent removal of the unreacted ferricyanide with a DE52 (Whatman) column. The purity of cyt *c* was confirmed by the ratio of the absorbance at 409 nm to that at 280 nm (Abs_{409}/Abs_{280} > 4.1). Molar extinction coefficients of WT and mutant human cyt *c* were determined by the hemochrome method.[43] The concentration of cyt *c* was adjusted by the intensity of its Soret band.

Refolding of Cyt *c*. Purified oxidized monomeric horse and human cyt *c* (0.02−2.3 mM) in the unfolded state were obtained by addition of GdnHCl (final concentrations of 3.5−6.5 M) in 50 mM potassium phosphate buffer (pH 7.0). Refolding of cyt *c* was performed by two methods.

Desalting Column Method. Refolding was performed by removing GdnHCl from the oxidized cyt *c* solution with a desalting gel column (PD SpinTrap G-25, GE Healthcare) without changing the cyt *c* concentration significantly. The column was washed four times with 400 μL of 50 mM potassium phosphate buffer (pH 7.0) by centrifugation (800*g*) for 1 min and subsequently incubated at the experimental temperature for 30 min before being used. Approximately 100−140 μL of the cyt *c* solution containing GdnHCl was added to the column, and the contents were subsequently subjected to centrifugation (800*g*) for 2 min, yielding folded cyt *c*. The dilution factor for the desalting gel column was ∼1.1. Because the folding of cyt *c* occurred while the solution passed through the column, the actual dilution factor was even smaller than this value, and thus, we used the initial cyt *c* concentration before the desalting experiment for analysis.

Rapid Mixing Method. Refolding of cyt *c* was performed by diluting oxidized cyt *c* containing 3.5−6.5 M GdnHCl in 50 mM potassium phosphate buffer (pH 7.0) with the same buffer at 1:6 ratios using a rapid mixer (SM10003, Unisoku, Osaka, Japan) (mixing dead time of 1−2 ms) at 4 °C. The two pistons of the mixer were loaded with cyt *c* containing 3.5−6.5 M GdnHCl and the dilution buffer, respectively. The remaining GdnHCl in the cyt *c* solution obtained after the dilution was removed with the desalting gel column (PD SpinTrap G-25, GE Healthcare).

dx.doi.org/10.1021/bi400986g | *Biochemistry* 2013, 52, 8732−8744

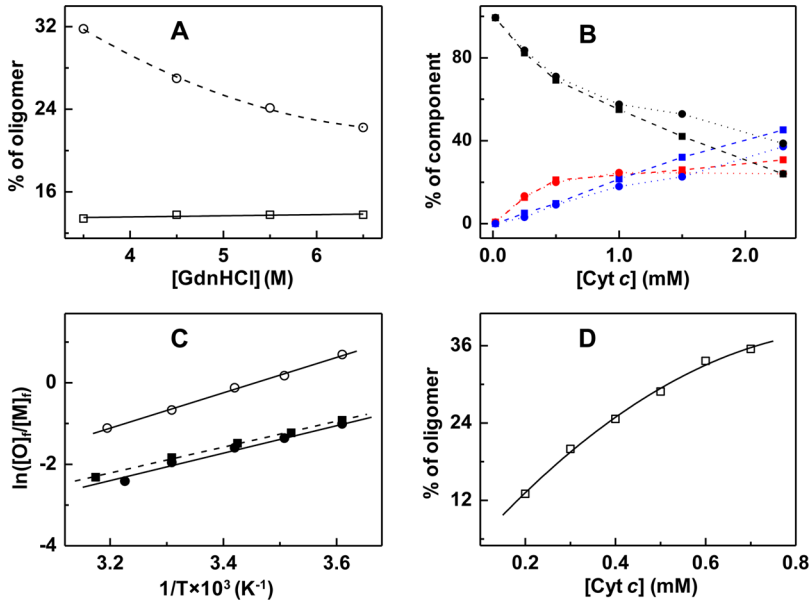

Figure 1. Oxidized monomeric and oligomeric horse and human cyt *c* obtained by folding. (A) Percentage of oligomeric horse cyt *c* obtained by refolding from the unfolded state in 50 mM potassium phosphate buffer (pH 7.0) containing 3.5−6.5 M GdnHCl with the desalting (—□—) and rapid mixing (---○---) methods. GdnHCl was removed from the 0.2 mM unfolded cyt *c* buffer solution during the desalting method at 4 °C. For the rapid mixing folding method, 1.4 mM cyt *c* in buffer containing GdnHCl was diluted with the buffer to 0.2 mM cyt *c* at 4 °C (1:6 mixture). (B) Folding at different cyt *c* concentrations by the desalting method at 4 °C: monomer (black), dimer (red), and sum of trimer and higher-order oligomers (blue) of horse (circles with dotted lines) and human cyt *c* (squares with dashed lines). (C) Natural logarithm of the ratio between the concentrations of oxidized oligomeric and monomeric cyt *c* [$\ln([O]_f/[M]_f)$] obtained by folding with the desalting method at various temperatures for 0.85 mM horse cyt *c* (—●—), 0.85 mM human cyt *c* (---■---), and 2.3 mM horse cyt *c* (—○—). (D) Percentage of oligomeric horse cyt *c* obtained by refolding with the desalting method at 4 °C at different cyt *c* concentrations from the unfolded state containing 6.5 M GdnHCl. The error for each data point is ±3%.

Size Exclusion Chromatographic Analysis. The amount of oxidized oligomeric cyt *c* in the solution was analyzed by size exclusion chromatography with a Superdex 75 10/300 GL gel column (GE Healthcare) using the FPLC system (BioLogic DuoFlow 10, Bio-Rad) [flow rate of 0.5 mL/min, monitoring wavelength of 409 nm, solvent of 50 mM potassium phosphate buffer (pH 7.0), and temperature of 4 °C]. The elution curves were fit with a multipeak Gaussian fitting procedure (Origin 8, OriginLab Corp.). The intensity of the peak area of the dimer or higher-order oligomers was divided by a value of 1.1, because the absorbance at 409 nm of the dimer or higher-order oligomers was 1.1 times larger than that of the monomer. The percentages of the monomer and oligomer were obtained by dividing the normalized area of the peak in the elution curve by the total area of the peaks.

Preparation of Dimeric Cyt *c*. Concentrated (0.5−2.3 mM) oxidized monomeric horse or human cyt *c* was unfolded by addition of 5.0−6.5 M GdnHCl in 50 mM potassium phosphate buffer (pH 7.0). Refolding was performed with the desalting column (PD SpinTrap G-25, GE Healthcare). The dimers were purified by gel chromatography (Hiload 26/60 Superdex 75, GE Healthcare) using the FPLC system (BioLogic DuoFlow 10, Bio-Rad) [flow rate of 0.8 mL/min, monitoring wavelength of 409 nm, solvent of 50 mM potassium phosphate buffer (pH 7.0), and temperature of 4 °C].

X-ray Crystallography. Crystallization was conducted at 277 K using the sitting drop vapor diffusion method with a crystal screening kit (Emerald Biosystems Inc.). The protein concentration was 50 mg/mL in 50 mM Tris-HCl buffer (pH 7.4). The droplet prepared by mixing 1 μL of the protein solution with 1 μL of the reservoir solution was equilibrated. The reservoir solution consisted of 40% PEG 200, 200 mM $(NH_4)_2HPO_4$, and 0.1 M Tris-HCl buffer (pH 8.0).

The preliminary structure was obtained by a molecular replacement method (MOLREP) using the atomic coordinates of the structure of horse cyt *c* (PDB entry 1HRC) as a starting model. Structural refinement was performed using REFMAC. The molecular model was manually corrected, and water molecules were picked up in the electron density map using COOT. The data collection and refinement statistics are summarized in Table S2 of the Supporting Information.

Optical Absorption and CD Measurements. Absorption spectra were recorded with a UV-2450 spectrophotometer (Shimadzu, Kyoto, Japan) using a 1 cm path-length quartz cell at 20 °C. CD spectra were recorded with a J-725 CD spectrophotometer (Jasco, Kyoto, Japan) using a 0.1 cm path-length quartz cell at 20 °C. Protein solutions in 50 mM potassium phosphate buffer (pH 7.0) were filtered through a 0.45 μm filter (Millex, Millipore, Bedford, MA) before measurements.

SAXS Measurements. All samples were prepared in 50 mM potassium phosphate buffer (pH 7.0). SAXS measurements were taken using a rotating anode X-ray generator, UltraX18 (Rigaku), in which a monochromatic X-ray with a wavelength of 1.54 Å was focused through a confocal Max-Flux mirror (Rigaku). Scattering profiles were collected using an X-ray image intensifier CCD detector (Hamamatsu Photonics K.K.). The sample cell with a path length of 0.1 cm was controlled at 10 °C. We measured a series of monomer and dimer dilutions, which were used to eliminate interparticle interference by extrapolation to zero protein concentration. Surface envelope models were calculated using GASBOR[44] after the treatment of the scattering profile with GNOM.[45] The

dx.doi.org/10.1021/bi400986g | *Biochemistry* 2013, 52, 8732−8744

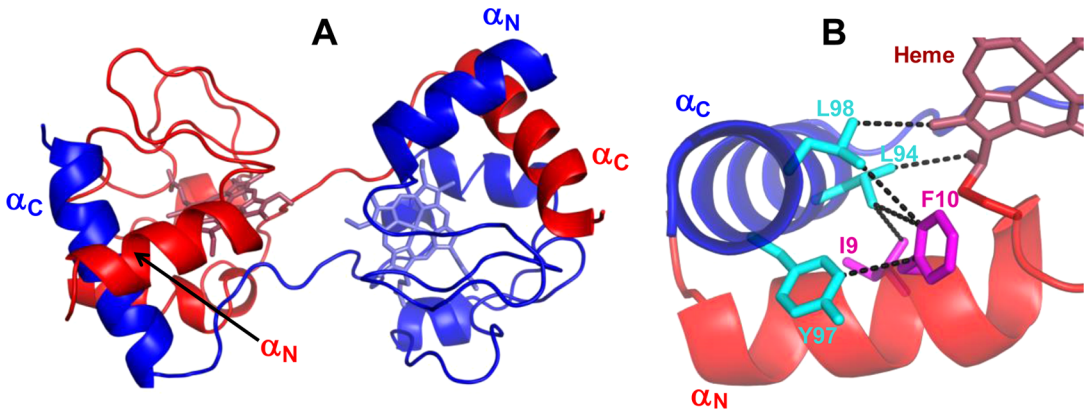

Figure 2. Crystal structure of oxidized dimeric horse cyt *c* obtained by refolding with the desalting method. (A) Structure of dimeric cyt *c* (red and blue) (PDB entry 3WC8). (B) Expanded view with the interactions between the hydrophobic amino acid residues of the N- and C-terminal α-helices. The heme is shown as raspberry sticks. I9 and F10 (pink) and L94, Y97, and L98 (cyan) are shown as sticks. N-Terminal (red) and C-terminal (blue) helices are labeled α_N and α_C, respectively.

average structure was obtained after superimposing the 30 independently calculated models.

Change in Absorbance during Folding of Cyt *c*. Changes in absorbance around 695 nm during folding of oxidized horse cyt *c*, WT human cyt *c*, and a mixture of I9G and L98G human cyt *c* mutants were monitored with rapid-scan stopped-flow equipment (RSP-601-03, Unisoku). Unfolded oxidized horse (0.3 or 3.0 mM) or human (0.3 mM) cyt *c* containing 3.5 M GdnHCl in 50 mM potassium phosphate buffer (pH 7.0) was diluted with the same buffer at a 1:2 ratio using the rapid mixer (SM10003, Unisoku) (mixing dead time of 1−2 ms) at 12 °C. The absorption spectra after mixing with an interval of 0.04 s were measured until 20 s had elapsed. An average of 10 independent measurements at each concentration was performed. The time profiles were calculated for the difference in the intensities of the absorption between 695 and 750 nm. The time profiles obtained for horse cyt *c* at high and low protein concentrations were least-squares fitted by global fitting with biexponential functions with the same rate constants but different intensities (Origin 8). The time profiles of WT human cyt *c* and a mixture of human cyt *c* mutants were fit by the same procedure.

RESULTS

Oligomerization of Cyt *c*. Oxidized horse monomeric cyt *c* (0.2 mM) was unfolded via an addition of GdnHCl (3.5−6.5 M) and refolded using 50 mM potassium phosphate buffer (pH 7.0). Refolding was performed by two methods: (1) with a desalting spin column to remove GdnHCl from the solution without changing the protein concentration significantly and (2) with a rapid mixer (mixing dead time of 1−2 ms) to rapidly reduce the GdnHCl concentration. Dimeric and trimeric cyt *c* proteins were detected in the elution curves of size exclusion chromatography, in addition to the monomer for both refolding methods (Figure S1 of the Supporting Information). These results show that cyt *c* oligomerizes during folding.

Oxidized horse cyt *c* formed ∼14% (heme unit) of oligomers when 3.5−6.5 M GdnHCl was removed from the cyt *c* (0.2 mM) solution with the desalting column at 4 °C (Figure 1A and Figure S1A of the Supporting Information). The amount of oligomers produced during refolding did not vary much with the initial GdnHCl concentration when they were refolded with the desalting column, because the cyt *c* concentration did not change significantly during the folding process. However, more oligomers were obtained when oxidized horse cyt *c* was refolded with the rapid mixer for the case in which the protein concentration after completion of mixing was the same as that of the desalting method, 0.2 mM (Figure 1A and Figure S1B of the Supporting Information). The extent of formation of oligomeric cyt *c* decreased from ∼32 to ∼22% (heme unit) in the solution when the initial GdnHCl concentration was increased from 3.5 to 6.5 M for folding with the rapid mixer at 4 °C. Cyt *c* may start to refold when the GdnHCl concentration decreases below the threshold of unfolding of the protein. When using the rapid mixer, the GdnHCl concentration may have decreased below the threshold before mixing was complete after 1−2 ms, and oligomerization may occur within its mixing dead time. Therefore, the actual cyt *c* concentration during the protein folding process was presumably higher than the final cyt *c* concentration (0.2 mM) after the completion of mixing, and the actual folding of cyt *c* occurred at a lower protein concentration in the case of higher initial GdnHCl concentrations. Because the amount of oligomers obtained by the rapid mixer method varied with the initial GdnHCl concentration, we used the desalting method for the analytical studies and the rapid mixing method for the kinetic studies.

We performed X-ray crystallographic analysis to investigate the structure of dimeric horse cyt *c*. The 1.8 Å resolution structure of dimeric horse cyt *c* obtained by folding with the desalting column exhibited a domain-swapped structure, where the C-terminal α-helix in the dimer was relocated from its original position observed in the monomer (PDB entry 3WC8) (Figure 2A). The dimeric cyt *c* structure presented here was similar to the structure of the dimer obtained by treatment with ethanol,[6] although some changes were observed in the hinge loop region, because of its structural flexibility. These results show that domain-swapped oligomers of horse cyt *c* are generated by folding from its unfolded state. The hydrophobic amino acid residues in the N-terminal α-helix and/or the heme of a protomer of dimeric cyt *c* were in the proximity of the hydrophobic residues in the C-terminal α-helix of the other protomer (Figure 2B), indicating that intermolecular hydrophobic interactions between the N- and C-terminal helices are important for the formation of dimeric cyt *c* during folding.

Effects of Cyt *c* Concentration and Temperature on Oligomerization. The swapping region of dimeric *Hydro-*

dx.doi.org/10.1021/bi400986g | *Biochemistry* 2013, 52, 8732−8744

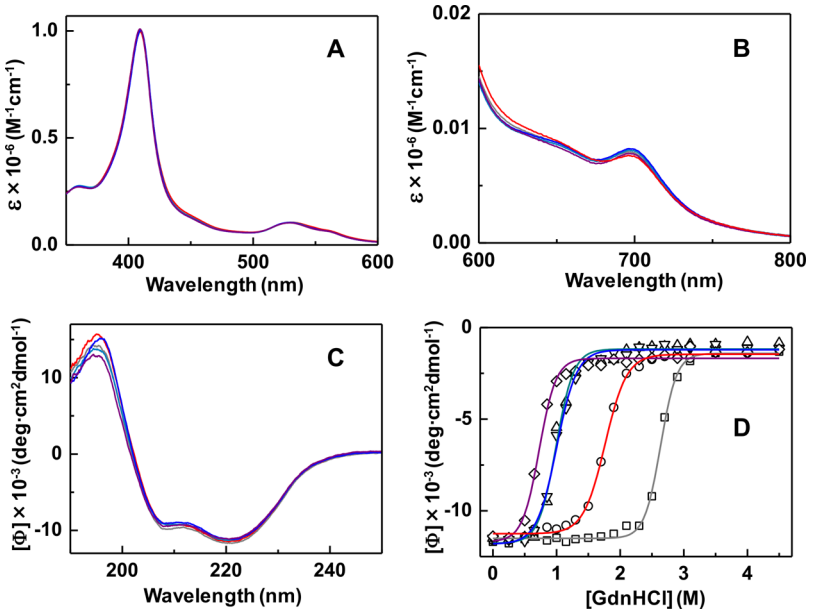

Figure 3. Optical absorption and CD spectra and stability of oxidized monomeric WT and mutant human cyt *c*. Optical absorption spectra in the (A) 350−600 nm and (B) 600−800 nm regions and (C) CD spectra in the 190−250 nm region of monomeric cyt *c*. Spectra of WT (gray), I9G (red), L94G (cyan), Y97G (blue), and L98G (purple) human cyt *c* are shown in panels A−C. (D) CD ellipticity of monomeric cyt *c* at 222 nm in the presence of GdnHCl: WT (□, gray), I9G (○, red), L94G (△, cyan), Y97G (▽, blue), and L98G (◇, purple). The midpoint GdnHCl concentrations for the folding−unfolding transition of WT, I9G, L94G, Y97G, and L98G were 2.7, 1.8, 1.0, 1.0, and 0.8 M, respectively. Protein concentrations of (A, C, and D) 10 μM (heme) and (B) 100 μM (heme).

genobacter thermophilus (HT) cytochrome c_{552} (cyt c_{552}) is different from that of dimeric horse cyt *c*.[6,46] The oligomerization properties are also different between horse cyt *c* and HT cyt c_{552}; i.e., high-order oligomers were detected in horse cyt *c*, whereas only tetramers and lower-order compounds were detected in HT cyt c_{552}.[6,46] We investigated the effects of protein concentration and temperature on oligomerization during folding of horse and human cyt *c*, where the amino acid sequence of human cyt *c* is 88% identical to that of horse cyt *c* and human cyt *c* exhibits a three-dimensional structure similar to that of horse cyt *c* (PDB entries 1HRC and 3NWV). Size exclusion chromatographic analyses showed that the amount of oxidized horse and human cyt *c* oligomers increased from ∼1 to ∼62% and from ∼1 to ∼76% (heme unit), respectively, when the protein concentration was increased from 0.02 to 2.3 mM for folding in 50 mM potassium phosphate buffer (pH 7.0) at 4 °C (Figure 1B and Figure S2 of the Supporting Information). These results strongly indicate that formation of domain-swapped oligomers of cyt *c* during folding is an intermolecular process for both horse and human cyt *c*.

When the temperature during folding was increased from 4 to 40 °C, the amount of oligomers formed by folding of 0.85 mM horse or human cyt *c* decreased from ∼42 to ∼11% (heme unit) for both proteins and from ∼62 to ∼24% (heme unit) for folding of 2.3 mM horse cyt *c* (Figure S3 of the Supporting Information). These results show that the intermolecular interaction for oligomer formation is favored at low temperatures over the intramolecular interaction for the formation of monomers. The plots of the logarithmic value of the dimer over monomer concentration versus the inverse of temperature exhibited linear correlations for both horse and human cyt *c* (Figure 1C). These results show that horse and human cyt *c* exhibit similar oligomerization properties, because of the similarity of the protein structures.

Oligomerization of N- and C-Terminal α-Helical Mutant Cyt *c*. Formation of N- and C-terminal α-helices and subsequent association of these helices by hydrophobic interaction occur early in the process of cyt *c* folding.[47−49] To elucidate the effect of intermolecular interaction between the N- and C-terminal α-helices of cyt *c* on oligomer formation during folding, we investigated folding of N- and C-terminal α-helical mutants of cyt *c* with reduced hydrophobicities. The dimeric horse cyt *c* structure revealed that hydrophobic residues Ile9 and Phe10 and the heme in the N-terminal region are in the proximity of hydrophobic residues Leu94, Tyr97, and/or Leu98 in the C-terminal region (Figure 2B). It has been shown in the monomeric structures of horse and human cyt *c* that Ile9 of the N-terminal α-helix is in the proximity of the amino acids in the C-terminal α-helix, and Tyr97 and Leu98 of the C-terminal α-helix are in the proximity of the amino acids in the N-terminal α-helix or the heme (PDB entries 1HRC and 3NWV).[1−3,50] It has also been reported that Leu94 of the C-terminal α-helix of horse cyt *c* plays a critical role for the N- and C-terminal α-helical interaction at the initial stage of folding.[32] In addition, Ile9, Phe10, Leu94, Tyr97, and Leu98 are all conserved between horse and human cyt *c*. Therefore, we constructed I9G, L94G, Y97G, and L98G mutants of human cyt *c*. Although Phe10 exhibits the most profound interhelical contacts, purification of a Phe10 mutant with reduced hydrophobicity was not successful, probably because removal of Phe10 was crucial for folding to its native structure. The optical absorption and CD spectra of these cyt *c* mutants in the oxidized form corresponded well to those of the WT protein (Figure 3A−C), indicating that the monomeric structures of these mutants were similar to that of WT cyt *c*. However, the protein stability against GdnHCl of these mutants decreased significantly compared to that of the WT protein, because of the decreased hydrophobicities at the N- or C-terminal α-helix (Figure 3D).

dx.doi.org/10.1021/bi400986g | *Biochemistry* 2013, 52, 8732−8744

WT and I9G human cyt *c* formed oligomers during folding for ~31 and ~26% (heme unit), respectively, by removal of 6.5 M GdnHCl at 4 °C with a desalting column (Figure 4 and Table 1). Only ~2 and ~1% (heme unit) of dimers were detected for L94G and Y97G cyt *c*, respectively, by folding under the same conditions, and no dimer was detected for L98G cyt *c*. These results show that the amount of oligomer formation decreases as the stability of the monomer decreases (Figures 3D and 4 and Table 1). The decrease in the extent of formation of oligomers for mutant cyt *c* compared to that for WT cyt *c* indicates that the hydrophobic interaction between the N- and C-terminal α-helices is important for the formation of oligomers during folding.

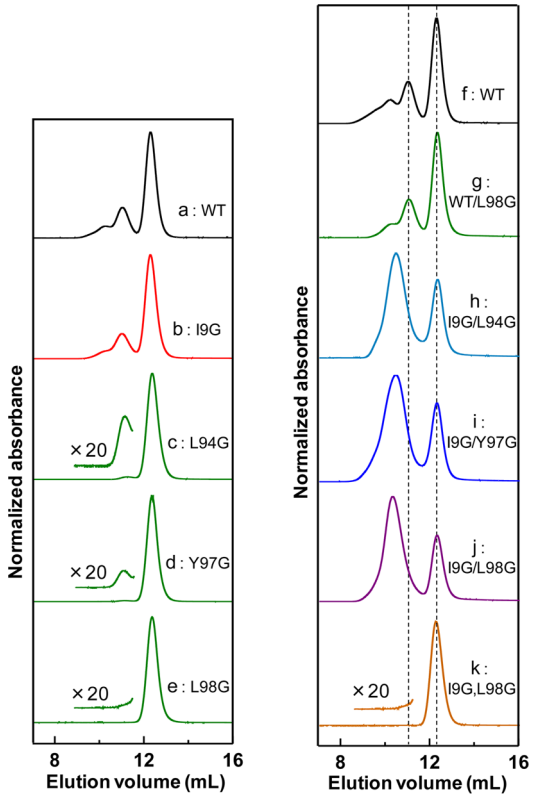

Figure 4. Size exclusion chromatography after folding of oxidized WT and mutant human cyt *c* and a mixture of two mutant forms of cyt *c*. Cyt *c* was refolded with the desalting method from the unfolded states in 50 mM potassium phosphate buffer (pH 7.0) containing 6.5 M GdnHCl at 4 °C: (a) WT, (b) I9G, (c) L94G, (d) Y97G, (e) L98G (concentration of 0.5 mM for parts a–e), (f) WT (1.0 mM), (g) WT/L98G, (h) I9G/L94G, (i) I9G/Y97G, and (j) I9G/L98G (concentration of 0.5 mM for each protein for parts g–j). The elution curve of a mixture of I9G (0.5 mM) and L98G (0.5 mM) cyt *c* after they had been incubated together at 4 °C for 10 h is shown in part k. The elution curves for the dimer regions in parts c–e and k are expanded 20-fold. The peak positions in the elution curve for monomeric (12.4 mL) and dimeric (11.0 mL) WT human cyt *c* are represented as black dotted lines in parts f–k. The intensities of the curves are normalized by the highest absorbance.

Folding was conducted with different combinations of WT and mutant cyt *c* in equal amounts: WT/N-terminal α-helical mutant, WT/C-terminal α-helical mutant, and N-terminal α-helical mutant/C-terminal α-helical mutant. Approximately 44% (heme unit) of the proteins formed oligomers during folding of a mixture of WT (0.5 mM) and I9G cyt *c* (0.5 mM).

Table 1. Amounts of Oligomers Formed by Folding of Oxidized WT and Mutant Human Cyt *c* and Their Mixture with the Desalting Method at 4 °C

	cyt *c*[a] (mM)	oligomer[b] (%)
WT	0.5	31
WT	1.0	44
I9G	0.5	26
L94G	0.5	2.1
Y97G	0.5	0.7
L98G	0.5	0.0
WT/I9G	0.5/0.5	44
WT/L98G	0.5/0.5	34
I9G/L94G	0.5/0.5	67
I9G/Y97G	0.5/0.5	71
I9G/L98G	0.5/0.5	71

[a]Concentration of each component. [b]Dimer and higher-order oligomers. The error for each data point is ±3%.

For the folding of a mixture of WT (0.5 mM) and L98G cyt *c* (0.5 mM), one may expect ~15.5% of the proteins to form oligomers, because 31% (heme unit) of the proteins formed oligomers by folding of 0.5 mM WT cyt *c* at 4 °C while L98G cyt *c* produced no oligomer (Figure 4 and Table 1). However, ~34% (heme unit) of the proteins formed oligomers during folding of a mixture of WT (0.5 mM) and L98G cyt *c* (0.5 mM) (Figure 4 and Table 1). No oligomer formed during incubation of folded WT and L98G cyt *c* together in the same buffer at 4 °C for 10 h (data not shown). These results indicate that L98G cyt *c* interacts with WT cyt *c* during folding, forming heterodimers in addition to WT cyt *c* homo-oligomers. Interestingly, when the N- and C-terminal mutants (I9G/L94G, I9G/Y97G, and I9G/L98G; 0.5 mM each) were folded together, many dimers (67–71%, heme unit) were produced compared to the number produced by folding of 1.0 mM WT cyt *c* (44%, heme unit) (Figure 4 and Table 1). The increase in the amount of dimers strongly suggests that the interaction of the N-terminal α-helix of L94G, Y97G, or L98G cyt *c* with the C-terminal α-helix of I9G cyt *c* has an essential role in oligomerization. In addition, the elution volume of the dimer during gel chromatography shifted largely from 11.0 mL for the WT and mutant cyt *c* homodimer to 10.4–10.6 mL for the I9G/L94G, I9G/Y97G, and I9G/L98G cyt *c* heterodimers (Figure 4). No peak was detected at the elution volume of the WT cyt *c* dimer. These results indicate that the heterodimer was the main species for the 1:1 mixture of the N- and C-terminal mutants. The smaller elution volume for the heterodimers suggests more open structures for the heterodimers than for the WT or I9G homodimer. The open structural property for the heterodimer was also detected in the SAXS measurement (see below). No dimer formed by incubation of folded I9G and L98G cyt *c* together in 50 mM potassium phosphate buffer (pH 7.0) at 4 °C for 10 h (Figure 4, curve k). These results support the hypothesis that the oligomers form during folding.

Characterization of Homo- and Heterodimers of N- and C-Terminal α-Helical Mutant Cyt *c*. The absorption maximum of the Soret band of the oxidized WT human cyt *c* dimer blue-shifted to 406.5 nm with an increase in intensity of ~10% compared to that of the monomer band at 409.5 nm (Figure 5A). Similar absorption properties of the Soret band were detected for other homo- and heterodimers of N- and C-terminal α-helical mutant human cyt *c*. The intensity of the 695

dx.doi.org/10.1021/bi400986g | *Biochemistry* 2013, 52, 8732–8744

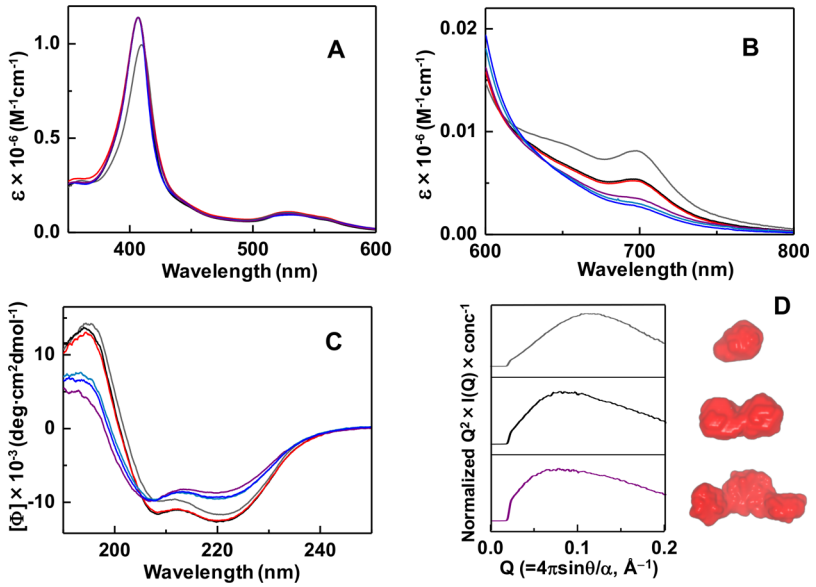

Figure 5. Optical absorption and CD spectra and SAXS curves shown by Kratky plots of oxidized monomeric and dimeric WT and mutant human cyt *c*. Optical absorption spectra in the (A) 350−600 nm and (B) 600−800 nm regions and (C) CD spectra in the 190−250 nm region of dimeric cyt *c*: WT (black) and I9G (red) homodimers and I9G/L94G (cyan), I9G/Y97G (blue), and I9G/L98G (purple) heterodimers. The gray line represents the spectrum of monomeric WT cyt *c*. (D) Small-angle X-ray scattering curves of monomeric (gray) and dimeric WT cyt *c* (black) and the heterodimer of I9G and L98G cyt *c* (purple). Surface envelopes of monomeric and dimeric cyt *c* obtained from the scattering curves are shown at the right. The intensities of the curves are normalized by the highest intensity. Protein concentrations of (A and C) 10 μM (heme), (B) 100 μM (heme), and (D) 1.0 mM (heme).

nm band, characteristic of Met80−heme coordination, decreased considerably in the oxidized WT human cyt *c* dimer compared to that of its monomer (Figure 5B), indicating that the Met−heme coordination was perturbed significantly in the dimer. Similar changes in the absorption spectra have been observed in dimeric horse cyt *c*.[6] However, although Met80 was not bound to the heme in the crystal structure of dimeric horse cyt *c* (Figure S4 of the Supporting Information), Met80 in a dimer may be in equilibrium between dissociated and associated forms to the heme iron in solution, because the 695 nm absorption band was observed with a lower intensity (Figure 5B).[6] The intensity of the 695 nm band in the oxidized I9G human cyt *c* dimer was also weaker than that of the band in the oxidized WT or I9G human cyt *c* monomer, whereas the intensity decreased significantly for all the heterodimers of N- and C-terminal mutant cyt *c* (Figure 5B). These results indicate that the Met80−heme coordination in these heterodimers is considerably perturbed compared to that of WT and I9G cyt *c* homodimers, presumably because of the flexibility of the overall protein structure for the heterodimers.

The intensities of the negative 208 nm band in the CD spectra of both oxidized WT and I9G cyt *c* homodimers were slightly larger than those of their monomers (Figure 5C). These results demonstrate a slight perturbation in the secondary structure of these dimers compared to that of the monomer. The intensities of the 208 and 222 nm CD bands for the I9G/L94G, I9G/Y97G, and I9G/L98G cyt *c* heterodimers were reduced significantly compared to those of the WT and I9G cyt *c* homodimers (to ∼70% for the 222 nm band) (Figure 5C), indicating that heterodimers are partially unfolded.

According to the SAXS measurements, the oxidized WT human cyt *c* dimer exhibited a structure with two globular units connected to each other (Figure 5D). The solution structure of dimeric human cyt *c* revealed by SAXS measurement was similar to that reported for the horse cyt *c* dimer.[6] The I9G/L98G heterodimer exhibited a size of 2.3mer, which consisted of a globular unit with two small, unfolded units beside it. The fact that the I9G/L98G heterodimer was larger than the WT dimer was consistent with the observation of smaller elution volumes for the heterodimers in size exclusion chromatography (Figure 4, curves h−j). The globular unit may be formed by the interaction of the C-terminal helix of I9G cyt *c* with the N-terminal helix of L98G cyt *c*, and the mutated N- and C-terminal α-helices may not interact with each other. Intermolecular interaction between the native N-terminal α-helix of the C-terminal mutant and the native C-terminal α-helix of the N-terminal mutant may be stronger than the intermolecular interaction containing a mutated amino acid, and the native interaction may become dominant during folding. In fact, ∼7 and ∼73% (heme unit) of the WT homodimer and the I9G/L98G heterodimer dissociated to monomers, respectively, after incubation at 47 °C for 30 min, whereas the I9G homodimer dissociated completely to monomers with the same treatment (Figure 6). These results show that the I9G/L98G heterodimer is more stable than the I9G homodimer, presumably because the heterodimer may contain one strong intermolecular hydrophobic interaction between the N- and C-terminal α-helices, whereas the I9G homodimer may contain two but only weak interactions between helices. The high stability of the WT dimer is due to the two strong nativelike intermolecular hydrophobic interactions between the unmodified N- and C-terminal α-helices.

Methionine Coordination during Folding of Cyt *c* at Different Protein Concentrations. The Met80−heme iron bond formation process during the final folding step of oxidized horse and human cyt *c* was investigated by monitoring the intensity change of the 695 nm absorption band related to the Met80−heme coordination. The Met80−heme coordination process was monitored at different protein concentrations: 0.1 mM (low concentration) and 1.0 mM (high concentration).

dx.doi.org/10.1021/bi400986g | *Biochemistry* 2013, 52, 8732−8744

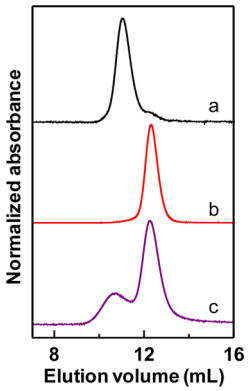

Figure 6. Size exclusion chromatography of oxidized dimeric WT and mutant human cyt *c*. The cyt *c* solution was analyzed after incubation of the dimers at 47 °C for 30 min: (a) WT dimer, (b) I9G dimer, and (c) heterodimer of I9G and L98G cyt *c*. The intensities of the curves are normalized by the highest absorbance.

The intensity of the 695 nm band increased gradually with time by rapid mixing of denatured cyt *c* (0.3 or 3.0 mM) in 50 mM potassium phosphate buffer (pH 7.0) containing 3.5 M GdnHCl with the same buffer at 12 °C (1:2 mixing) (Figure 7A,B). The concentration of cyt *c* decreased to 0.1 or 1.0 mM and that of GdnHCl to 1.17 M after mixing. The increase in absorption at 695 nm in horse cyt *c* was observed mainly within 2 s for folding at low protein concentrations, whereas the change was still observable after 10 s for folding at high concentrations. To determine the folding rate constants, absorbance differences between 695 and 750 nm were plotted versus time after mixing (Figure 7C). A biexponential behavior was identified for the changes in the absorbance differences at both low and high cyt *c* concentrations with rate constants of 2.8 ± 0.2 and 0.27 ± 0.01 s^{-1}, respectively (Table 2), although the percentage of the slower phase increased from ~22 to ~58% with the increase in the cyt *c* concentration from 0.1 to 1.0 mM.

A biexponential behavior was also identified for the change in absorption during folding of oxidized WT human cyt *c* or a mixture of I9G and L98G human cyt *c* mutants at 0.1 mM, although the rate constants (1.8 ± 0.2 and 0.19 ± 0.1 s^{-1}) were slightly lower than those of horse cyt *c*. The percentages of the slower phase during folding of oxidized WT human cyt *c* and a mixture of I9G and L98G human cyt *c* mutants were estimated to be ~31 and ~85%, respectively (Table 2). A large decrease in the overall absorption change for the mixture of I9G and L98G cyt *c* mutants was observed (Figure 7D), because of a large decrease in the intensity of the 695 nm band for the heterodimer (Figure 5B).

DISCUSSION

More oligomers formed with an increase in protein concentration during folding of horse or human cyt *c* (Figure 1B), indicating that the oligomerization is an intermolecular process and is competitive with a monomeric folding process. The produced dimeric horse cyt *c* exhibited a domain-swapped structure, in which the C-terminal α-helix was exchanged between protomers (Figure 2). These results suggest that both

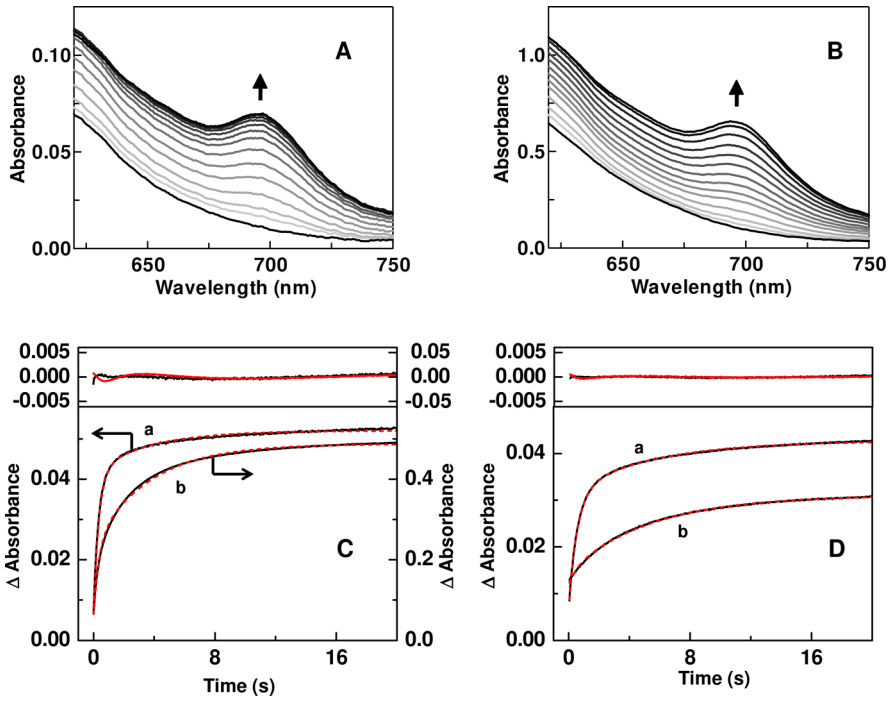

Figure 7. Changes in the 695 nm absorption band of oxidized cyt *c* during folding. (A and B) Folding of oxidized horse cyt *c* at (A) 0.3 and (B) 3.0 mM in buffer containing 3.5 M GdnHCl diluted to one-third by the rapid mixing method (1:2 mixing). Absorption spectra 0.0, 0.04, 0.08, 0.16, 0.28, 0.40, 0.60, 0.92, 1.4, 2.0, 3.0, 5.0, 9.0, and 15.0 s after mixing are shown. (C) Time courses of the difference absorption between 695 and 750 nm of horse cyt *c* at (a) 0.1 and (b) 1.0 mM (concentrations after mixing). (D) Time courses of the difference absorption between 695 and 750 nm of human cyt *c* at 0.1 mM: (a) WT and (b) 1:1 mixture of I9G and L98G cyt *c*. The red dashed lines in panels C and D represent the least-squares-fitted biexponential curves. Residuals of the fitted curves are shown in the top sections of panels C (black for 0.1 mM horse cyt *c* (left axis) and red for 1.0 mM horse cyt *c* (right axis)) and D (black for WT human cyt *c* (left axis) and red for 1.0 mM horse cyt *c*). Protein concentrations (after mixing) of (A) 0.1 and (B) 1.0 mM.

dx.doi.org/10.1021/bi400986g | *Biochemistry* 2013, 52, 8732–8744

Table 2. Folding Rate Constants of Oxidized Horse and WT and Mutant Human Cyt *c* at Different Protein Concentrations Obtained by the Rapid-Scan Stopped-Flow Mixing Method at 12 °C[a]

	[cyt *c*] (mM)[b]				
	initial	final	rate constant (s^{-1})	amplitude (%)	estimated amount of oligomers[c] (%)
horse	0.3	0.1	2.8 ± 0.2	78 ± 2	31
			0.27 ± 0.01	22 ± 2	
	3.0	1.0	2.8 ± 0.2	42 ± 2	69
			0.27 ± 0.01	58 ± 2	
WT human	0.3	0.1	1.8 ± 0.2	69 ± 2	40
			0.19 ± 0.01	31 ± 2	
I9G and L98G human[d]	0.3	0.1	1.8 ± 0.2	15 ± 2	93
			0.19 ± 0.01	85 ± 2	

[a]The adjusted R^2 value of the fit was 0.998 for all measurements. [b]Protein concentration during refolding. [c]Values estimated from kinetic amplitudes. The amplitudes of the slow phase for horse cyt *c*, WT human cyt *c*, and the mixture of I9G and L98G human cyt *c* were multiplied by 1.6, 1.5, and 2.4, respectively, because the absorbance at 695 nm of the monomer was larger than that of the corresponding oligomer. [d]Mixing of 0.15 mM I9G human cyt *c* and 0.15 mM L98G human cyt *c* was performed.

horse and human cyt *c* form domain-swapped oligomers by folding from their denatured states. The amount of oligomeric cyt *c* obtained during folding with the rapid mixing method decreased with an increase in the initial GdnHCl concentration, suggesting that folding of cyt *c* and its oligomerization may occur at the same GdnHCl concentration within the mixing dead time of the mixer (1−2 ms). The cyt *c* concentration when folding proceeded via the rapid mixing method can be estimated by comparison of the amount of oligomers formed between the rapid mixing and desalting methods. Because ∼32% of horse cyt *c* formed oligomers by folding from the solution containing 3.5 M GdnHCl with the rapid mixing method (Figure 1A and Figure S1B of the Supporting Information), the actual cyt *c* concentration when folding occurred for this condition was estimated to be 0.55 mM from Figure 1D. Approximately 22% of horse cyt *c* formed oligomers using the rapid mixing method by folding from the unfolded state with 6.5 M GdnHCl, and the actual cyt *c* concentration was estimated from Figure 1D to be 0.33 mM when folding occurred. By assuming that the GdnHCl was diluted to the same extent as cyt *c*, we estimated folding of cyt *c* occurred at approximately 1.4−1.5 M GdnHCl for all the initial GdnHCl concentrations studied. In fact, most of the cyt *c* molecules exist in the folded state at this GdnHCl concentration according to the folding titration against the GdnHCl concentration.[51,52] Oligomerization of cyt *c* may have occurred at the nascent stage of folding within the mixing dead time when the N- and C-terminal α-helices of partially folded proteins interacted intermolecularly (Figure 8), because the amount of oligomers depended on the actual cyt *c* concentrations when folding occurred. The distribution of the size of oligomeric horse cyt *c* produced by folding from the solution containing 3.5 M GdnHCl with the rapid mixing method (estimated cyt *c* concentration during folding of 0.55 mM) was similar to that produced by folding of 0.5 mM horse cyt *c* with the rapid mixing method (curve a of Figure S1B of the Supporting Information and curve c of Figure S2A of the Supporting Information). These results show that the oligomerization and the distribution of the size of the oligomers may not depend on the folding method (the desalting or rapid mixing method), but rather on the condition of the solution.

Because oligomers may form through dimers (Figure 8), we may interpret that the monomer and oligomers (dimer and higher-order oligomers) form with intramolecular and intermolecular interactions, respectively, by the following equations.

$$\text{monomer: } d[M]/dt = k_M[U_M] \quad (1)$$

$$\text{oligomer: } d[O]/dt = k_O[U_M]^2 \quad (2)$$

where [M] and [O] represent the concentrations of the folded monomer and oligomer, respectively, and $[U_M]$ represents the concentration of the unfolded protein. We defined the rate constants for formation of the folded monomer and oligomer as

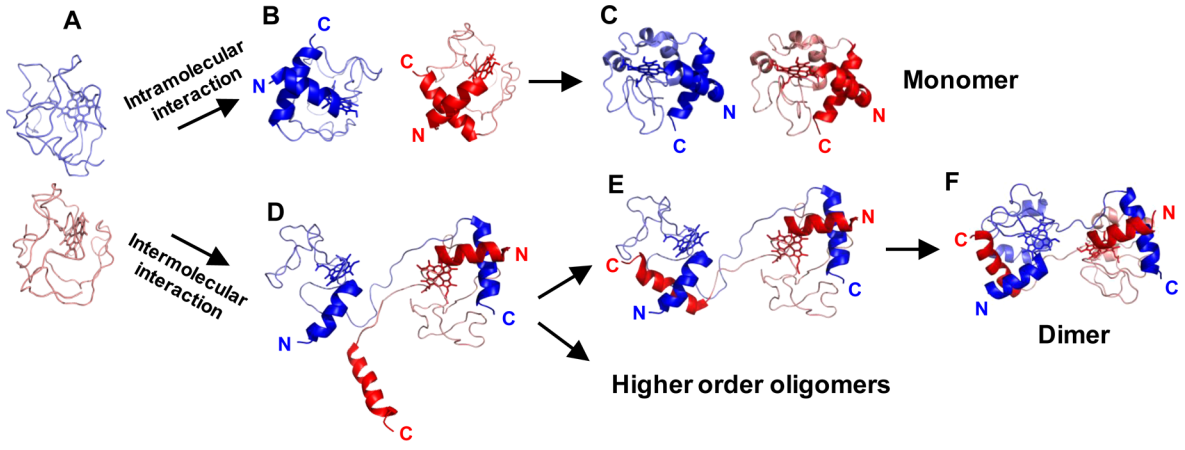

Figure 8. Schematic view of folding of cyt *c* and formation of its dimer. (A) Model of unfolded cyt *c*. (B) Model of monomer intermediates with intramolecular interaction between the N- and C-terminal α-helices. (C) Structure of monomeric cyt *c* (PDB entry 1HRC). (D) Model of the oligomer intermediate with intermolecular interaction between an N-terminal α-helix and a C-terminal α-helix. (E) Model of the dimer intermediate with intermolecular interaction between the N- and C-terminal α-helices. (F) Structure of dimeric cyt *c* (PDB entry 3WC8) determined in this study. N- and C-terminal α-helices and the hemes of the two cyt *c* molecules are colored red and blue, whereas the rest of the protein is shown in pale colors.

dx.doi.org/10.1021/bi400986g | *Biochemistry* 2013, 52, 8732−8744

k_M and k_O, respectively. We neglected the interaction of the intermediate dimer and unfolded monomer. Because the value of d([O]/[M])/dt is proportional to $[U_M]$ throughout the reaction, we may obtain

$$[O]_f/[M]_f = k_O/k_M \times \int_0^{[U_M]_0} [U_M]\, d[U_M] / \int_0^{[U_M]_0} d[U_M] = k_O[U_M]_0/2k_M \quad (3)$$

where $[M]_f$ and $[O]_f$ represent the final concentrations of the folded monomer and oligomer, respectively, and $[U_M]_0$ denotes the initial value of $[U_M]$, and thus, we obtain

$$k_O/k_M = 2[O]_f/([M]_f[U_M]_0) \quad (4)$$

Although each folding rate constant of the monomer (k_M) and oligomer (k_O) was difficult to deduce, the ratio of the rate constants of the oligomer and monomer (k_O/k_M) was determined to be $(1.5 \pm 0.3) \times 10^3$ M^{-1} for all the cyt c concentrations studied.

If we assume the Arrhenius relationship for the folding reactions

$$\text{monomer: } k_M = A_M \exp[-E_M/(RT)] \quad (5)$$

$$\text{oligomer: } k_O = A_O \exp[-E_O/(RT)] \quad (6)$$

where E_M and E_O represent the activation energies for folding of the monomer and oligomer, respectively, and we obtain

$$\ln([O]_f/[M]_f) = \ln[(k_O[U_M]_0)/(2k_M)] = -(E_O - E_M)/(RT) + \ln[A_O/(2A_M)] + \ln[U_M]_0 \quad (7)$$

where A_M and A_O represent the pre-exponential factors for the folding of the monomer and oligomer, respectively, and T and R represent the temperature and gas constant, respectively. The slope in the plot of $\ln([O]_f/[M]_f)$ versus $1/T$ represents $-(E_O - E_M)/R$, which was positive under the conditions studied, indicating $E_M > E_O$ (Figure 1C). The slope of the plot was similar between different protein concentrations, indicating that the difference in the activation energy between folding of monomeric and oligomeric cyt c is not affected significantly by the protein concentration. The intercept difference of 1.2 between the plots for 0.85 and 2.3 mM cyt c corresponded well to the value of $\log[U_M]_0$ (ln 2.3 − ln 0.85 = 1.0).

It has been reported that the hydrophobicities of the N- and C-terminal α-helices play a critical role in the kinetics of cyt c folding (Figure 8).[32] The dimeric horse cyt c structure also indicates that N- and C-terminal hydrophobic contacts are essential for domain swapping (Figure 2B). Reduction of the hydrophobicity in the N- or C-terminal α-helix in mutant cyt c may weaken the intramolecular and intermolecular hydrophobic interactions between the N- and C-terminal helices during folding. In fact, folding of cyt c to oligomers was suppressed in the N- and C-terminal α-helical mutants (Figure 4). We investigated the folding of a mixture of N- and C-terminal human cyt c mutants, where a large amount of the heterodimers was obtained with a negligible amount of higher-order oligomers. The strong intermolecular hydrophobic interaction between the N-terminal α-helix of the C-terminal mutant and the C-terminal α-helix of the N-terminal mutant predominates over the intermolecular and intramolecular interactions between the native N-terminal α-helix and the mutated C-terminal α-helix (and between the native C-terminal α-helix and the mutated N-terminal α-helix). Therefore, formation of the heterodimer became more favorable than formation of monomers and homodimers.

The elution volumes of all the heterodimers studied were smaller than that of the WT cyt c dimer (Figure 4), suggesting that the interaction between the two mutated terminal α-helices becomes weaker and the overall protein size becomes larger in the heterodimers. Approximately 30% of the α-helical structures was unfolded in the heterodimer compared to the WT cyt c dimer according to CD measurements (Figure 5C), and a slightly larger size compared to that of the WT cyt c dimer was detected for the heterodimer of I9G and L98G cyt c in the SAXS measurements (Figure 5D). The larger size of the heterodimer was presumably caused by its partially unfolded structure, which was also suggested from the CD measurements. The formation of higher-order oligomers may also be inhibited by the decrease in the level of intermolecular interaction between the mutated helices. Therefore, folding of a mixture of N- and C-terminal mutants resulted in a large amount of heterodimers. These results strongly support the hypothesis that the intermolecular hydrophobic interaction between the N- and C-terminal α-helices guides cyt c to form oligomers during folding.

A slow folding phase (time constant of ~3 s) of cyt c has been reported at high protein concentrations,[53] and a transient dimer has been detected in its refolding kinetics by SAXS measurements.[39] In the folding of horse cyt c in the presence of 1.17 M GdnHCl, the intensities of the fast (~400−500 ms) and slow (~4−5 s) phases for the amplitude change of the 695 nm band differed with protein concentration (Figure 7C and Table 2). A higher ratio of the slow phase was observed at higher protein concentrations, indicating that this phase may be due to the formation of the Met80−heme bond during folding of oligomers, whereas the fast phase represents the formation of the Met80−heme bond during folding of the monomers. The ratio between monomeric and oligomeric horse cyt c for the difference absorption between 695 and 750 nm is 1.6:1.[6] By considering the difference in intensity at 695 nm between monomeric and oligomeric cyt c, the amount of oligomers formed by folding at 0.1 and 1.0 mM cyt c was deduced to be 31 and 69%, respectively. These results show that the oligomerization may affect the formation of the Met80−heme bond during folding of cyt c, where the ratio of the oligomers depends on the protein concentration. The amounts of oligomers produced by folding at 0.1 mM cyt c for WT human cyt c and a 1:1 mixture of I9G and L98G human cyt c mutants were estimated in a similar way to be 40 and 93%, respectively (Figure 7D and Table 2), where the intensity ratios of the absorption at 695 nm of monomeric and oligomeric cyt c were deduced from their absorption spectra to be 1.5:1 and 2.4:1 for WT human cyt c and the mixture of I9G and L98G human cyt c mutants, respectively (Figures 3B and 5B). The production of a small amount of monomers by folding from the mixture of I9G and L98G human cyt c mutants was consistent with the results of size exclusion chromatography (Figure 4, curve j). However, the amount of oligomers deduced from the change in kinetics of horse and human cyt c was greater than those obtained by gel chromatographic analysis, although the temperature was slightly higher for the kinetic measurements than for the gel chromatographic analysis (Figure 1B and Table 2). The differences were presumably caused by dissociation of

dx.doi.org/10.1021/bi400986g | Biochemistry 2013, 52, 8732−8744

the oligomer to monomers in the presence of 1.17 M GdnHCl after folding had reached completion.

The heme of cyt *c* in the guanidinium (Gdn) ion unfolded state at neutral pH is reported to be bis-His-coordinated.[37] The difference in the biphasic nature between the monomer and oligomer may be due to the difference in the amount of proteins folding from a misligated species to the His/Met-ligated native species. Because the absorption at ~625 nm, which is attributed to the absorption of a H_2O-coordinated high-spin species,[54−56] did not change significantly during folding (Figure 7A,B), the misligated form may be mainly the bis-His-coordinated species. The unfolded state of cyt *c* is reported to make a contribution to the stability of the protein.[57] Equilibrium studies of Gdn ion-unfolded yeast iso-1-cyt *c* showed that intermolecular His26−heme dimers occur in 3 M GdnHCl at pH <5.0 at relatively low protein concentrations.[58] The amount of cyt *c* oligomers obtained by folding with the desalting method decreased by more than 50% when the pH was decreased from 7.0 to 4.0 (Figure S5 of the Supporting Information), where the amount of bis-His-coordinated species of the unfolded state decreases.[37] These results show that certain amount of domain-swapped dimers may be formed from the bis-His-coordinated species in the unfolded state. The intensity of the 695 nm band of horse and human cyt *c* homodimers was smaller than the intensity of the band of their monomers (Figure 5B),[6] indicating a weaker coordination of Met80 to the heme iron in the oligomers than in the monomers. Therefore, the coordination of Met80 to the heme iron may be slower in the oligomer than in the monomer in the folding of cyt *c*. Although detailed experiments are necessary to elucidate the ligand properties of oligomers during the folding of cyt *c*, our results strongly indicate that the slow folding phase is caused by the intermolecular hydrophobic interaction forming domain-swapped oligomers.

■ CONCLUSION

Domain-swapped dimeric cyt *c* was obtained by folding from the Gdn ion-induced unfolded state. The amount of oligomers formed by the refolding of cyt *c* increased with an increase in protein concentration and a decrease in temperature. A large amount of heterodimers was obtained by the folding of a mixture of N- and C-terminal α-helical mutant cyt *c* with decreased hydrophobicities. This heterodimer was more unfolded than the WT cyt *c* dimer. These results strongly indicate that oligomeric cyt *c* is formed by intermolecular hydrophobic interaction between the N- and C-terminal α-helices. The contribution of a slow phase increased in the folding process of cyt *c* at high protein concentrations, corresponding to the ligand exchange process forming the Met80−heme bond in the domain-swapped oligomer.

■ ASSOCIATED CONTENT

Supporting Information

Nucleotide sequences of primers, statistics of data collection, size exclusion chromatography, structures, and a crystal structure. This material is available free of charge via the Internet at http://pubs.acs.org.

■ AUTHOR INFORMATION

Corresponding Author

*Phone: +81-743-72-6110. Fax: +81-743-72-6119. E-mail: hirota@ms.naist.jp.

Present Address

⊥H. Komori: Faculty of Education, Kagawa University, 1-1 Saiwai-cho, Takamatsu, Kagawa 760-8522, Japan.

Funding

This work was partially supported by Grants-in-Aid for Scientific Research from MEXT [Priority Areas, 23107723 (S.H.)], JSPS [Category B, 21350095 (S.H.)], the Sankyo Foundation of Life Science (S.H.), the Toray Science Foundation (S.H.), and Photo Factory, KEK [2010G091 and 2012G043 (H. Komori)]. P.P.P. acknowledges support from Department of Science and Technology (DST), GOI, under a BOYSCAST fellowship (SR/BY/C-08/10).

Notes

The authors declare no competing financial interest.

■ ACKNOWLEDGMENTS

We thank Dr. Zhonghua Wang (Nara Institute of Science and Technology) for the construction of the human cyt *c* plasmid. We are also grateful to Mr. Leigh McDowell (Nara Institute of Science and Technology) for his advice on the preparation of the manuscript. We also thank the staff at beamline BL44XU Spring-8, JAPAN (Proposal No. 2012B6720). The MX225-HE (Rayonix) CCD detector at BL44XU was financially supported by Academia Sinica and by the National Synchrotron Radiation Research Center (Taiwan, ROC).

■ ABBREVIATIONS

cyt *c*, cytochrome *c*; Gdn, guanidinium; GdnHCl, guanidine hydrochloride; CD, circular dichroism; SAXS, small-angle X-ray scattering; PCR, polymerase chain reaction; CCHL, cyt *c* heme lyase; WT, wild-type; PDB, Protein Data Bank; HT, *Hydrogenobacter thermophilus*; cyt c_{552}, cytochrome c_{552}.

■ REFERENCES

(1) Dickerson, R. E., Takano, T., Eisenberg, D., Kallai, O. B., Samson, L., Cooper, A., and Margoliash, E. (1971) Ferricytochrome *c*. I. General features of the horse and bonito proteins at 2.8 Å resolution. *J. Biol. Chem. 246*, 1511−1535.

(2) Bushnell, G. W., Louie, G. V., and Brayer, G. D. (1990) High-resolution three-dimensional structure of horse heart cytochrome *c*. *J. Mol. Biol. 214*, 585−595.

(3) Banci, L., Bertini, I., Gray, H. B., Luchinat, C., Reddig, T., Rosato, A., and Turano, P. (1997) Solution structure of oxidized horse heart cytochrome *c*. *Biochemistry 36*, 9867−9877.

(4) Li, P., Nijhawan, D., Budihardjo, I., Srinivasula, S. M., Ahmad, M., Alnemri, E. S., and Wang, X. (1997) Cytochrome *c* and dATP-dependent formation of Apaf-1/caspase-9 complex initiates an apoptotic protease cascade. *Cell 91*, 479−489.

(5) Spierings, D., McStay, G., Saleh, M., Bender, C., Chipuk, J., Maurer, U., and Green, D. R. (2005) Connected to death: The (unexpurgated) mitochondrial pathway of apoptosis. *Science 310*, 66−67.

(6) Hirota, S., Hattori, Y., Nagao, S., Taketa, M., Komori, H., Kamikubo, H., Wang, Z., Takahashi, I., Negi, S., Sugiura, Y., Kataoka, M., and Higuchi, Y. (2010) Cytochrome *c* polymerization by successive domain swapping at the C-terminal helix. *Proc. Natl. Acad. Sci. U.S.A. 107*, 12854−12859.

(7) Wang, Z., Matsuo, T., Nagao, S., and Hirota, S. (2011) Peroxidase activity enhancement of horse cytochrome *c* by dimerization. *Org. Biomol. Chem. 9*, 4766−4769.

(8) Soffer, J. B., Fradkin, E., Pandiscia, L. A., and Schweitzer-Stenner, R. (2013) The (not completely irreversible) population of a misfolded state of cytochrome *c* under folding conditions. *Biochemistry 52*, 1397−1408.

(9) Newcomer, M. E. (2002) Protein folding and three-dimensional domain swapping: A strained relationship? *Curr. Opin. Struct. Biol. 12*, 48−53.
(10) Rousseau, F., Schymkowitz, J. W., and Itzhaki, L. S. (2003) The unfolding story of three-dimensional domain swapping. *Structure 11*, 243−251.
(11) Bennett, M. J., Sawaya, M. R., and Eisenberg, D. (2006) Deposition diseases and 3D domain swapping. *Structure 14*, 811−824.
(12) Gronenborn, A. M. (2009) Protein acrobatics in pairs: Dimerization via domain swapping. *Curr. Opin. Struct. Biol. 19*, 39−49.
(13) Janowski, R., Kozak, M., Jankowska, E., Grzonka, Z., Grubb, A., Abrahamson, M., and Jaskolski, M. (2001) Human cystatin C, an amyloidogenic protein, dimerizes through three-dimensional domain swapping. *Nat. Struct. Biol. 8*, 316−320.
(14) Staniforth, R. A., Giannini, S., Higgins, L. D., Conroy, M. J., Hounslow, A. M., Jerala, R., Craven, C. J., and Waltho, J. P. (2001) Three-dimensional domain swapping in the folded and molten-globule states of cystatins, an amyloid-forming structural superfamily. *EMBO J. 20*, 4774−4781.
(15) Knaus, K. J., Morillas, M., Swietnicki, W., Malone, M., Surewicz, W. K., and Yee, V. C. (2001) Crystal structure of the human prion protein reveals a mechanism for oligomerization. *Nat. Struct. Biol. 8*, 770−774.
(16) Guo, Z., and Eisenberg, D. (2006) Runaway domain swapping in amyloid-like fibrils of T7 endonuclease I. *Proc. Natl. Acad. Sci. U.S.A. 103*, 8042−8047.
(17) Liu, C., Sawaya, M. R., and Eisenberg, D. (2011) β_2-Microglobulin forms three-dimensional domain-swapped amyloid fibrils with disulfide linkages. *Nat. Struct. Mol. Biol. 18*, 49−55.
(18) Liu, Y., Gotte, G., Libonati, M., and Eisenberg, D. (2001) A domain-swapped RNase A dimer with implications for amyloid formation. *Nat. Struct. Biol. 8*, 211−214.
(19) Liu, Y., Gotte, G., Libonati, M., and Eisenberg, D. (2002) Structures of the two 3D domain-swapped RNase A trimers. *Protein Sci. 11*, 371−380.
(20) Liu, Y., Hart, P. J., Schlunegger, M. P., and Eisenberg, D. (1998) The crystal structure of a 3D domain-swapped dimer of RNase A at a 2.1-Å resolution. *Proc. Natl. Acad. Sci. U.S.A. 95*, 3437−3442.
(21) Gotte, G., Vottariello, F., and Libonati, M. (2003) Thermal aggregation of ribonuclease A. A contribution to the understanding of the role of 3D domain swapping in protein aggregation. *J. Biol. Chem. 278*, 10763−10769.
(22) López-Alonso, J. P., Bruix, M., Font, J., Ribó, M., Vilanova, M., Rico, M., Gotte, G., Libonati, M., González, C., and Laurents, D. V. (2006) Formation, structure, and dissociation of the ribonuclease S three-dimensional domain-swapped dimer. *J. Biol. Chem. 281*, 9400−9406.
(23) López-Alonso, J. P., Bruix, M., Font, J., Ribó, M., Vilanova, M., Jiménez, M. A., Santoro, J., González, C., and Laurents, D. V. (2010) NMR spectroscopy reveals that RNase A is chiefly denatured in 40% acetic acid: Implications for oligomer formation by 3D domain swapping. *J. Am. Chem. Soc. 132*, 1621−1630.
(24) Jerala, R., and Žerovnik, E. (1999) Accessing the global minimum conformation of stefin A dimer by annealing under partially denaturing conditions. *J. Mol. Biol. 291*, 1079−1089.
(25) Rousseau, F., Schymkowitz, J. W., Wilkinson, H. R., and Itzhaki, L. S. (2001) Three-dimensional domain swapping in p13suc1 occurs in the unfolded state and is controlled by conserved proline residues. *Proc. Natl. Acad. Sci. U.S.A. 98*, 5596−5601.
(26) Liu, L., Byeon, I. J., Bahar, I., and Gronenborn, A. M. (2012) Domain swapping proceeds via complete unfolding: A ^{19}F- and ^{1}H-NMR study of the Cyanovirin-N protein. *J. Am. Chem. Soc. 134*, 4229−4235.
(27) Zegers, I., Deswarte, J., and Wyns, L. (1999) Trimeric domain-swapped barnase. *Proc. Natl. Acad. Sci. U.S.A. 96*, 818−822.
(28) Koharudin, L. M., Liu, L., and Gronenborn, A. M. (2013) Different 3D domain-swapped oligomeric cyanovirin-N structures suggest trapped folding intermediates. *Proc. Natl. Acad. Sci. U.S.A. 110*, 7702−7707.
(29) Nagao, S., Osuka, H., Yamada, T., Uni, T., Shomura, Y., Imai, K., Higuchi, Y., and Hirota, S. (2012) Structural and oxygen binding properties of dimeric horse myoglobin. *Dalton Trans. 41*, 11378−11385.
(30) Wu, L. C., Laub, P. B., Elove, G. A., Carey, J., and Roder, H. (1993) A noncovalent peptide complex as a model for an early folding intermediate of cytochrome *c*. *Biochemistry 32*, 10271−10276.
(31) Bai, Y., Sosnick, T. R., Mayne, L., and Englander, S. W. (1995) Protein folding intermediates: Native-state hydrogen exchange. *Science 269*, 192−197.
(32) Colón, W., Elöve, G. A., Wakem, L. P., Sherman, F., and Roder, H. (1996) Side chain packing of the N- and C-terminal helices plays a critical role in the kinetics of cytochrome *c* folding. *Biochemistry 35*, 5538−5549.
(33) Shastry, M. C., and Roder, H. (1998) Evidence for barrier-limited protein folding kinetics on the microsecond time scale. *Nat. Struct. Biol. 5*, 385−392.
(34) Elöve, G. A., Bhuyan, A. K., and Roder, H. (1994) Kinetic mechanism of cytochrome *c* folding: Involvement of the heme and its ligands. *Biochemistry 33*, 6925−6935.
(35) Takahashi, S., Yeh, S. R., Das, T. K., Chan, C. K., Gottfried, D. S., and Rousseau, D. L. (1997) Folding of cytochrome *c* initiated by submillisecond mixing. *Nat. Struct. Biol. 4*, 44−50.
(36) Yeh, S. R., Takahashi, S., Fan, B., and Rousseau, D. L. (1997) Ligand exchange during cytochrome *c* folding. *Nat. Struct. Biol. 4*, 51−56.
(37) Yeh, S. R., Han, S. W., and Rousseau, D. L. (1998) Cytochrome *c* folding and unfolding: A biphasic mechanism. *Acc. Chem. Res. 31*, 727−736.
(38) Elöve, G. A., Chaffotte, A. F., Roder, H., and Goldberg, M. E. (1992) Early steps in cytochrome *c* folding probed by time-resolved circular dichroism and fluorescence spectroscopy. *Biochemistry 31*, 6876−6883.
(39) Segel, D. J., Eliezer, D., Uversky, V., Fink, A. L., Hodgson, K. O., and Doniach, S. (1999) Transient dimer in the refolding kinetics of cytochrome *c* characterized by small-angle X-ray scattering. *Biochemistry 38*, 15352−15359.
(40) Pollock, W. B., Rosell, F. I., Twitchett, M. B., Dumont, M. E., and Mauk, A. G. (1998) Bacterial expression of a mitochondrial cytochrome *c*. Trimethylation of Lys72 in yeast iso-1-cytochrome *c* and the alkaline conformational transition. *Biochemistry 37*, 6124−6131.
(41) Wang, Z. H., Lin, Y. W., Rosell, F. I., Ni, F. Y., Lu, H. J., Yang, P. Y., Tan, X. S., Li, X. Y., Huang, Z. X., and Mauk, A. G. (2007) Converting cytochrome *c* into a peroxidase-like metalloenzyme by molecular design. *ChemBioChem 8*, 607−609.
(42) Dente, L., and Cortese, R. (1987) pEMBL: A new family of single-stranded plasmids for sequencing DNA. *Methods Enzymol. 155*, 111−119.
(43) Berry, E. A., and Trumpower, B. L. (1987) Simultaneous determination of hemes *a*, *b*, and *c* from pyridine hemochrome spectra. *Anal. Biochem. 161*, 1−15.
(44) Svergun, D. I. (1992) Determination of the regularization parameter in indirect-transform methods using perceptual criteria. *J. Appl. Crystallogr. 25*, 495−503.
(45) Svergun, D. I., Petoukhov, M. V., and Koch, M. H. (2001) Determination of domain structure of proteins from X-ray solution scattering. *Biophys. J. 80*, 2946−2953.
(46) Hayashi, Y., Nagao, S., Osuka, H., Komori, H., Higuchi, Y., and Hirota, S. (2012) Domain swapping of the heme and N-terminal α-helix in *Hydrogenobacter thermophilus* cytochrome c_{552} dimer. *Biochemistry 51*, 8608−8616.
(47) Maity, H., Maity, M., and Englander, S. W. (2004) How cytochrome *c* folds, and why: Submolecular foldon units and their stepwise sequential stabilization. *J. Mol. Biol. 343*, 223−233.
(48) Pletneva, E. V., Gray, H. B., and Winkler, J. R. (2005) Many faces of the unfolded state: Conformational heterogeneity in denatured yeast cytochrome *c*. *J. Mol. Biol. 345*, 855−867.

(49) Pletneva, E. V., Gray, H. B., and Winkler, J. R. (2005) Snapshots of cytochrome *c* folding. *Proc. Natl. Acad. Sci. U.S.A. 102*, 18397−18402.
(50) Liptak, M. D., Fagerlund, R. D., Ledgerwood, E. C., Wilbanks, S. M., and Bren, K. L. (2011) The proapoptotic G41S mutation to human cytochrome *c* alters the heme electronic structure and increases the electron self-exchange rate. *J. Am. Chem. Soc. 133*, 1153−1155.
(51) Pascher, T., Chesick, J. P., Winkler, J. R., and Gray, H. B. (1996) Protein folding triggered by electron transfer. *Science 271*, 1558−1560.
(52) Okuno, T., Hirota, S., and Yamauchi, O. (2000) Folding character of cytochrome *c* studied by *o*-nitrobenzyl modification of methionine 65 and subsequent ultraviolet light irradiation. *Biochemistry 39*, 7538−7545.
(53) Nawrocki, J. P., Chu, R. A., Pannell, L. K., and Bai, Y. (1999) Intermolecular aggregations are responsible for the slow kinetics observed in the folding of cytochrome *c* at neutral pH. *J. Mol. Biol. 293*, 991−995.
(54) Lu, Y., Casimiro, D. R., Bren, K. L., Richards, J. H., and Gray, H. B. (1993) Structurally engineered cytochromes with unusual ligand-binding properties: Expression of *Saccharomyces cerevisiae* Met-80 → Ala iso-1-cytochrome *c*. *Proc. Natl. Acad. Sci. U.S.A. 90*, 11456−11459.
(55) Bren, K. L., and Gray, H. B. (1993) Structurally engineered cytochromes with novel ligand-binding sites: Oxy and carbonmonoxy derivatives of semisynthetic horse heart Ala80 cvytochrome *c*. *J. Am. Chem. Soc. 115*, 10382−10383.
(56) Silkstone, G. G., Cooper, C. E., Svistunenko, D., and Wilson, M. T. (2005) EPR and optical spectroscopic studies of Met80X mutants of yeast ferricytochrome *c*. Models for intermediates in the alkaline transition. *J. Am. Chem. Soc. 127*, 92−99.
(57) Behera, R. K., Nakajima, H., Rajbongshi, J., Watanabe, Y., and Mazumdar, S. (2013) Thermodynamic effects of the alteration of the axial ligand on the unfolding of thermostable cytochrome *c*. *Biochemistry 52*, 1373−1384.
(58) Tzul, F. O., Kurchan, E., Roder, H., and Bowler, B. E. (2009) Competition between reversible aggregation and loop formation in denatured iso-1-cytochrome *c*. *Biochemistry 48*, 481−491.